

# Limitations of the Giant Spin Hamiltonian in Explaining Magnetization Tunneling in a Single-Molecule Magnet

A. Wilson,<sup>1</sup> J. Lawrence,<sup>1</sup> E.-C. Yang,<sup>2</sup> M. Nakano,<sup>3</sup> D. N. Hendrickson,<sup>2</sup> and S. Hill<sup>1</sup>,

<sup>1</sup>Department of Physics, University of Florida, Gainesville, FL 32611, USA

<sup>2</sup>Department of Chemistry and Biochemistry, University of California at San Diego, La Jolla, CA 92093-0358, USA

<sup>3</sup>Department of Applied Chemistry, Osaka University, Suita 565-0871, Japan  
(Dated: September 21, 2021)

EPR studies of a Ni<sub>4</sub> single-molecule magnet yield the zero-field-splitting (zfs) parameters, D, B<sub>4</sub><sup>0</sup> and B<sub>4</sub><sup>4</sup>, based on a giant spin approximation (GSA) with S = 4. Experiments on an isostructural Ni-doped Zn<sub>4</sub> crystal establish the Ni<sup>II</sup> ion zfs parameters. The 4<sup>th</sup>-order zfs parameters in the GSA arise from the interplay between the Heisenberg interaction, J<sub>ij</sub> S<sub>i</sub> · S<sub>j</sub>, and the 2<sup>nd</sup>-order single-ion anisotropy, giving rise to mixing of higher lying S ≠ 4 states into the S = 4 state. Consequently, J directly influences the zfs in the ground state, enabling its direct determination by EPR.

PACS numbers: 75.50.Xx, 75.60.Jk, 75.75.+a, 76.30.-v

The Ni(hmp)(ROH)Cl<sub>4</sub> molecule (abbreviated Ni<sub>4</sub>) possessing the ROH = dm b ligand (Ni<sub>4</sub><sup>dm b</sup> [1, 2, 3, 4, 5]) represents a model system for carefully examining the validity of the giant spin approximation (GSA) which has been widely applied in the study of single-molecule magnets (SMMs) [6]. The GSA assumes the total spin, S, of the molecule to be a good quantum number, and then models the lowest-lying (2S + 1) magnetic sub-levels in terms of an effective spin Hamiltonian of the form:

$$\hat{H} = D \hat{S}_z^2 + B_4^0 \hat{O}_4^0 + B_4^4 \hat{O}_4^4 + \sum_{ij} B_{ij} \hat{g} \cdot \hat{S}_i \quad (1)$$

The first three terms parameterize anisotropic magnetic interactions which lead to zero-field-splitting (zfs) of the ground-state multiplet (see red lines in Fig. 1 for the case of S = 4), e.g. spin-orbit coupling, dipolar interactions, etc; here, we consider only 2<sup>nd</sup> and 4<sup>th</sup>-order operators (see [6] for definitions) which are compatible with the S<sub>4</sub> symmetry of the Ni<sub>4</sub><sup>dm b</sup> SMM. The final term represents the Zeeman interaction associated with the application of a magnetic field, B, where  $\hat{g}$  is the Lande g-tensor.

SMMs are defined by a dominant 2<sup>nd</sup>-order uniaxial anisotropy, D S<sub>z</sub><sup>2</sup>, with D < 0 [6]. Nevertheless, weaker 4<sup>th</sup>-order terms have been shown to play a crucial role in the quantum dynamics of several high-symmetry SMMs (especially Mn<sub>12</sub>-acetate) [5, 7, 8, 9], even though the precise origin of these terms has not previously been understood [10]. In this letter, we show that higher order terms D(2n), n > 1 arise naturally in the GSA through the interplay between intrinsic magneto-anisotropy (at the sites of individual magnetic ions in the molecule) and inter-spin-state mixing (controlled by exchange). These findings raise questions concerning the validity of the GSA, particularly in terms of its predictive powers.

The Ni<sub>4</sub><sup>dm b</sup> SMM is particularly attractive for this investigation. The four s = 1 Ni<sup>II</sup> ions reside on opposing corners of a slightly distorted cube (Fig. 1 inset) [3, 4, 5]. DC susceptibility data (χ<sub>M</sub>T) indicate a relatively large

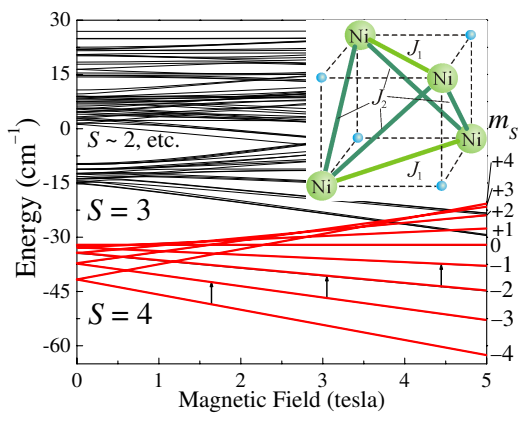


FIG. 1: Field dependence of the 81 eigenvalues corresponding to the four-spin Hamiltonian (Eq. 2). The lowest 9 levels (red lines) can be modeled by the GSA with S = 4 (Eq. 1). The inset shows a schematic of the cubic core of the Ni<sub>4</sub><sup>dm b</sup> SMM (the blue spheres represent O).

ground state spin of S = 4 for the molecule, and a reasonable separation (> 35 K) between this and higher lying states with S < 4 [3, 5]. These properties can be rationalized in terms of pure ferromagnetic coupling between the Ni<sup>II</sup> ions. In addition, efforts to fit low-temperature electron paramagnetic resonance (EPR) and magnetization data to the GSA (Eq. 1 and red lines in Fig. 1) have been highly successful [1, 2, 3]. Thus, Ni<sub>4</sub><sup>dm b</sup> displays all of the hallmarks of a SMM, yet it exhibits unusually fast magnetic quantum tunneling (MQT) at zero field [5].

The GSA assumes S to be rigid, thereby ignoring the internal magnetic degrees of freedom within a SMM which can give rise to couplings to higher-lying states (S mixing [11, 12]) that may ultimately influence MQT. A more physical model, which takes into account zfs interactions at the individual Ni<sup>II</sup> sites, as well as the exchange coupling between individual magnetic ions, is

given by the following Hamiltonian [1]:

$$\hat{H} = \sum_i \left[ P_i \hat{S}_i^z + \sum_{i,j} J_{ij} \hat{S}_i \cdot \hat{S}_j + \sum_i \left( d_i \hat{S}_{zi}^2 + e_i \hat{S}_{xi}^2 + \hat{S}_{yi}^2 + B \hat{S}_i^z + g_i \hat{S}_i \right) \right] \quad (2)$$

Here, the  $\hat{S}_i$  ( $= x; y; z$ ) represent spin projection operators, and  $\hat{S}_i$  the total spin operator, corresponding to the individual  $Ni^{II}$  ions;  $d_i$  ( $< 0$ ) and  $e_i$  respectively parameterize the uniaxial and rhombic zfs interactions in the local coordinate frame of each  $Ni^{II}$  ion; likewise,  $g_i$  represents the Lande  $g$ -tensor at each site; finally, the  $J_{ij}$  parameterize the isotropic exchange couplings between pairs of  $Ni^{II}$  ions.

For  $Ni_4^{dm b}$ , the dimension of the four-spin Hamiltonian matrix (Eq. 2) is just  $[(2s+1)^4]^2 = 81 \times 81$ , which is easily handled by any modern PC (in contrast to  $Mn_{12}$ -acetate which has dimension  $10^8 \times 10^8$  [13]). More importantly, the  $3 \times 3$  Hamiltonian matrix associated with a single  $Ni^{II}$  ion contains only two zfs parameters,  $d_i$  and  $e_i$  (in addition to  $g_i$ ). Furthermore, due to the high symmetry of the molecule, these matrices are related simply by the  $S_4$  symmetry operation, and the number of exchange constants reduces to just two ( $J_1$  and  $J_2$ , see Fig. 1 inset). Consequently, the four-spin model contains only a handful of parameters, each of which can be determined independently, often by more than one method [1, 2, 3, 4, 5]. Fig. 1 displays the 81 Zeeman-split eigenvalues corresponding to the four-spin Hamiltonian (Eq. 2), using parameters obtained from fits described later. The lowest nine levels are fairly well separated from higher lying states; these levels, which dominate the EPR spectrum, can be equally well described by the Hamiltonian corresponding to Eq. 1 with  $S = 4$  [1, 2, 3]. Roughly  $20 \text{ cm}^{-1}$  above this ground state multiplet exists a grouping of 21 levels which can reasonably be treated as three separate  $S = 3$  multiplets. There is then a gap to a more-or-less continuum of levels. The notion of a well defined spin quantum number becomes tenuous at this point.

There are a number of other important reasons why we chose to focus on the  $Ni_4^{dm b}$  member of the  $Ni_4$  family. To begin with,  $Ni^{II}$  is readily amenable to substitution with non-magnetic Zn. Thus, one can synthesize crystals of  $Zn_4^{dm b}$  lightly doped with  $Ni^{II}$  [4]. The result is a small fraction of predominantly  $s = 1$   $Zn_3Ni$  magnetic species diluted into a non-magnetic host crystal. X-ray studies indicate that the structures of the  $Ni_4^{dm b}$  and  $Zn_4^{dm b}$  complexes are virtually identical. Thus, EPR studies of the doped crystals provide very reliable estimates of the single-ion zfs parameters for  $Ni^{II}$  in the parent  $Ni_4^{dm b}$  compound ( $d_i$ ,  $e_i$  and  $g_i$  in Eq. 2) [4]. Another remarkable feature of the  $Ni_4^{dm b}$  member of the  $Ni_4$  family is that its structure contains absolutely no solvent of crystallization [3, 4, 5]. This is quite rare among SMMs, resulting

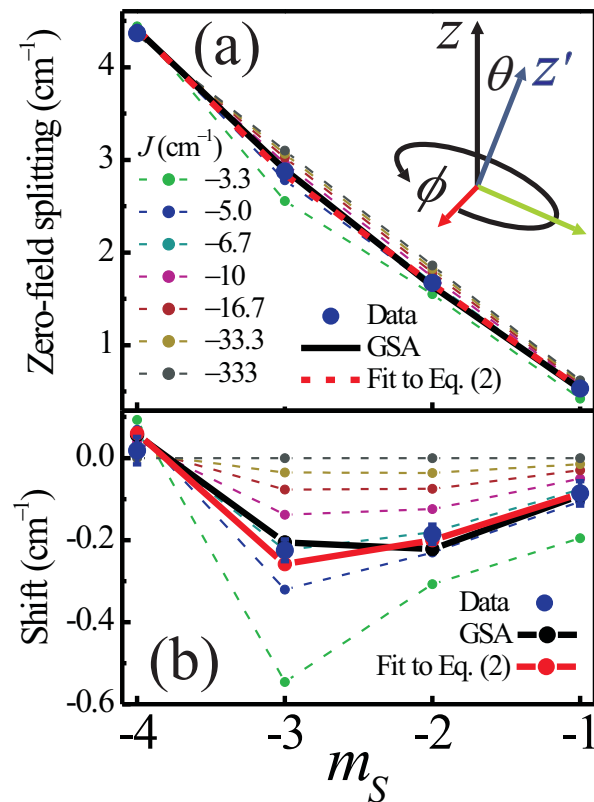


FIG. 2: (a)  $m_s$  dependence of the zfs energies [between  $m_s$  and  $(m_s + 1)$ ] within the ground state multiplet. The dashed curves show the zfs obtained from Eq. 2 as a function of  $J$ . The inset defines the Euler angles relating the  $Ni^{II}$  and molecular coordinates [4]. (b) Difference between the data in (a) and the  $J = -333 \text{ cm}^{-1}$  curve, emphasizing the non-linear  $m_s$  dependence of the zfs energies.

in the removal of a major source of disorder. Indeed, we believe that this is the primary reason why the  $Ni_4^{dm b}$  complex gives particularly sharp EPR spectra [14, 15]. In contrast, all of the other solvent containing  $Ni_4$  complexes exhibit rather broad EPR peaks [1]. Details of the experimental procedures, including representative EPR spectra, are presented elsewhere [2, 4, 17].

We begin by reviewing the results of single-crystal high-frequency EPR studies of  $Ni_4^{dm b}$  [1, 2, 3]. Based on an analysis using the GSA (Eq. 1), the lowest-lying  $S = 4$  multiplet is split by a dominant axial zfs interaction with  $D = 0.589(2) \text{ cm}^{-1}$ . In the absence of higher-order terms, this interaction produces a quadratic dependence of the  $(2S + 1)$  zero-field eigenvalues on the quantum number  $m_s$ , representing the projection of the total spin onto the easy-axis of the molecule. Consequently, the zfs between successive  $m_s$  levels should be linear in  $m_s$ . It is these splittings that one measures in an EPR experiment, albeit in a non-magnetic field. However, using a multi-frequency approach, one can ex-

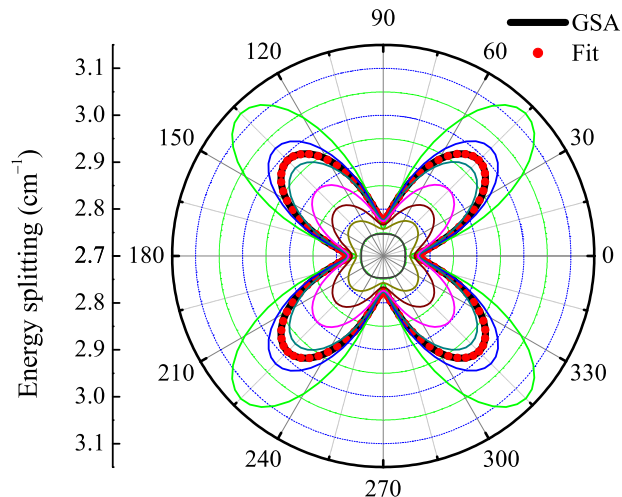


FIG. 3: Angle-dependence of the splitting of the lowest energy doublet ( $m_s = 4$  in zero-field) as a function of the field orientation within the hard plane. The thin curves are simulations using Eq. 2 with different  $J$  values (see Fig. 2 for color codes). The black and red data are the best fits to Eqns. 1 and 2, respectively.

extrapolate easy-axis data (B k z) to zero-field, yielding accurate determinations of these splittings [1]; these energy spacings are plotted versus  $m_s$  in Fig. 2 for  $Ni_4^{dm b}$ . As can be seen, the dependence of the zfs values on  $m_s$  is not linear. One can obtain agreement to within experimental error by including the 4<sup>th</sup>-order axial zfs interaction  $B_4^0 O_4^0$  ( $\hat{S}_z^4$ ) in the GSA, with  $B_4^0 = 1.2 \cdot 10^4 \text{ cm}^{-1}$  (black data in Fig. 2 [1]). The  $\hat{S}_z^4$  operator produces quartic  $m_s$  corrections to the zero-field eigenvalues and, thus, cubic corrections to the zfs, as seen in the figure. Unlike the 2<sup>nd</sup>-order term, which can easily be understood as originating from the 2<sup>nd</sup>-order zfs interactions at the individual  $Ni^{II}$  sites, the 4<sup>th</sup>-order term in the GSA does not have any obvious physical meaning. In this sense, it is nothing more than an adjustable parameter in an effective model (Eq. 1). As we will see below, this non-linear  $m_s$  dependence of the zfs values is directly related to S-mixing [11].

The four-fold ( $S_4$ ) symmetry of the  $Ni_4^{dm b}$  molecule forbids 2<sup>nd</sup>-order zfs interactions which break axial symmetry. Indeed, we find no evidence for such interactions based on EPR experiments conducted as a function of the field orientation within the hard plane. However, a very pronounced four-fold modulation of the spectrum is observed, which can be explained by the 4<sup>th</sup>-order  $B_4^4 O_4^4$  [ $\frac{1}{2} B_4^4 (\hat{S}_x^4 + \hat{S}_y^4)$ ] term in the GSA, with  $B_4^4 = 4 \cdot 10^4 \text{ cm}^{-1}$  [2]. Although this interaction is allowed by symmetry, it is not obvious how it relates to the underlying anisotropy associated with the individual  $Ni^{II}$  ions. Nevertheless, it does explain the fast MQT observed in this and other  $Ni_4$  complexes [2, 5]. When

treated as a perturbation to the axial zfs Hamiltonian,  $(\hat{S}_x^4 + \hat{S}_y^4)$  connects states that differ in  $m_s$  by 4 in first order and, therefore, lifts the degeneracy of the lowest lying  $m_s = 4$  states in 2nd order, leading to a tunnel splitting of order 10 MHz. This is an extremely large intrinsic tunnel splitting in comparison to other SMMs, and can be understood as arising because of the coincidence of the multiplicity of the ground state ( $2S + 1 = 9$ ) and the four-fold symmetry, which gives rise to a leading-order off-diagonal zfs interaction which is fourth order in the spin operators, i.e.  $(\hat{S}_x^4 + \hat{S}_y^4)$  is extremely effective at connecting the  $m_s = 4$  states.

We now attempt to understand the physical basis for the existence of the axial and transverse 4<sup>th</sup>-order zfs interactions ( $B_4^0 O_4^0$  and  $B_4^4 O_4^4$ ) deduced on the basis of the GSA. From previous studies of a Ni-doped  $Zn_4^{dm b}$  crystal, we determined not only the zfs parameters associated with the  $Ni^{II}$  ions, but also the orientations of the local magnetic axes associated with these interactions relative to the crystallographic axes [4]. However, the key point is that the Hamiltonian matrices for the individual  $S = 1$   $Ni^{II}$  ions have dimensions  $3 \times 3$ . Therefore, terms exceeding 2<sup>nd</sup>-order in the single-spin operators ( $\hat{S}_{ix}^2, \hat{S}_{iy}^2$ , etc.) are completely unphysical. If one assumes that the ground state for the  $Ni_4^{dm b}$  molecule corresponds to a rigid  $S = 4$  spin, one can then project the single-ion anisotropies onto the  $S = 4$  state using irreducible tensor operator methods [4]. However, after rotating from local to molecular coordinates, the projection is nothing more than a summation of the individual zfs matrices. Consequently, such a procedure does not produce terms of order four in the spin operators [4]. Therefore, the need to include 4<sup>th</sup>-order zfs interactions in an analysis of the EPR data for  $Ni_4^{dm b}$  may be taken as evidence for a breakdown of the GSA. We note that agreement in terms of the 2<sup>nd</sup>-order parameters is very good. In particular, the molecular D value agrees to within 10% with the value obtained from projection of the single-ion anisotropies onto the  $S = 4$  state [4]. In addition, although the single-ions experience a significant rhombic zfs interaction ( $e/d = 0.23$ ), symmetry considerations guarantee its cancellation when projected onto the  $S = 4$  state. Therefore, this approach is completely unable to account for the MQT in  $Ni_4^{dm b}$ .

In view of the above, one is forced to use a more realistic Hamiltonian (Eq. 2) which takes into account all spin states of the molecule. The isotropic exchange interaction,  $J_{ij}$ , in Eq. 2 connects states having the same spin-projection [12]. Consequently, it does not operate between states within a given spin multiplet, it simply lifts degeneracies between states with different multiplicity (see Fig. 1). The addition of anisotropic terms to Eq. 2 results in zfs within each multiplet which, in turn, gives rise to weaker  $m_s$ -dependent corrections to the exchange splittings. Thus, we see that  $J$  directly modifies the zfs energies within a given spin multiplet via interac-

tions (S-mixing) with nearby excited spin states. In the limit  $J \gg d$  one can expect these corrections to be negligible. However, in the present case, where  $J = d \approx 1.3$ , one can expect these corrections to be significant. Furthermore, since the corrections involve higher order processes whereby the underlying anisotropic interactions feedback into themselves via exchange coupling to nearby spin multiplets, it is clear that this will generate 'effective' interactions that are 4<sup>th</sup>-order (i.e. 2<sup>nd</sup>-order squared) in the spin operators (as well as higher order terms). However, these 4<sup>th</sup>-order interactions have no real physical basis other than that they arise due to the competing isotropic and anisotropic interactions in Eq. 2, resulting in S-mixing.

The influence of  $J$  on the lowest lying (nominally  $S = 4$ ) multiplet is abundantly apparent in Fig. 2, where we compare zfs energies determined via the four-spin Hamiltonian (Eq. 2) for different values of the exchange interaction strength, with those determined experimentally (blue data points) and from a fit to the experimental data using the GSA (Eq. 1, black data points). The magnitudes of  $d = 4.73 \text{ cm}^{-1}$  and  $e = 1.19 \text{ cm}^{-1}$  were established from combined fits to both easy-axis zfs data (red points in Fig. 2), and from hard-plane rotation measurements of the four-fold oscillation of the ground state splitting (Fig. 3, see also [2]). We made one simplifying assumption by setting  $J_1 = J_2 = J$ , based on DC M T data [16]. Regardless, this in no way invalidates the main conclusion of this letter: namely, that  $J$  influences the ground state zfs through S-mixing. The polar angle, (see Fig. 2 inset), between the local  $\text{Ni}^{II}$ -ion  $z$ -axes and the crystallographic  $z$ -axis was fixed at  $15^\circ$  on the basis of the Ni/Zn studies [4]. We additionally included a dipolar coupling (not shown in Eq. 2) between the four  $\text{Ni}^{II}$  ions using precise crystallographic data and no additional free parameters [11]. The remaining free parameters were  $g_x = g_y = 2.23$ ,  $g_z = 2.25$  and an additional Euler angle ( $\phi = 59^\circ$ ) illustrated in the inset to Fig. 2. A more in-depth account of the fitting procedure will be given elsewhere [17]. The obtained value of  $d$  agrees to within 12% with the value determined independently from measurements on the Ni-doped  $\text{Zn}_4$  crystal [ $d = 5.30(5) \text{ cm}^{-1}$ ]; the remaining parameters agree to within the experimental error [ $e = 1.20(2) \text{ cm}^{-1}$ ,  $g_x = g_y = 2.20(5)$ ,  $g_z = 2.30(5)$ ].

One can clearly see that, by reducing the separation between the ground  $S = 4$  multiplet and the lowest excited states (by reducing  $J$ ), one can reproduce both the nonlinear  $m_s$  dependence of the zfs energies (Fig. 2), which was attributed to the  $B_4^0$  term in the GSA [1], and the four-fold oscillation of the ground-state splitting observed from hard-plane measurements (Fig. 3), which was attributed to  $B_4^4$  [2]. This is quite a remarkable result, because it implies that one can deduce  $J$  directly from the spectroscopic information obtained via an EPR experiment. Indeed, the value of  $J = 5.9 \text{ cm}^{-1}$  de-

termined from these fits is in good agreement with the value of  $7.05 \text{ cm}^{-1}$  deduced on the basis of fits to M T data to Eq. 2 [16]. All of the apparent 4<sup>th</sup>-order behavior vanishes if one sets  $J \gg d$ , as expected in such a limit in which the ground state spin value is a good quantum number (due to the absence of S-mixing). In the opposite extreme ( $J \approx 3 \text{ cm}^{-1}$ ), we start to see evidence for even higher order corrections to the zfs energies (6<sup>th</sup> order). A cubic polynomial exhibits only one turning point (at  $m_s = 0.5$  in Fig. 2), whereas the green data in Fig. 2 clearly display more than one turning point when one recognizes that all of these curves must be antisymmetric about  $m_s = 0.5$ . Therefore, it is apparent that one should not limit the GSA to 4<sup>th</sup>-order terms for SMMs with relatively low-lying excited spin states. In fact, one cannot rule out equally good fits to experimental data which include 6<sup>th</sup> and higher-order zfs interactions. Consequently, one should be careful about making predictions on the basis of the GSA, particularly at vastly different energy scales compared to the experiments used to establish the GSA zfs parameters (e.g. EPR vs. MQT). Indeed, we find a difference of almost a factor of 10 between the ground-state tunnel splittings deduced from Eqs. 1 and 2 using the optimum zfs parameters for  $\text{Ni}_4^{\text{II}}$ . We note that the situation in  $\text{Ni}_4$  is not dissimilar to many other SMMs, including the most widely studied  $\text{Mn}_{12}$ -acetate, for which similar 4<sup>th</sup>-order zfs interactions and low-lying excited spin states are found [18, 19].

Finally, we note that the most unambiguous method for estimating exchange couplings in polynuclear metal complexes involves determining the exact locations of excited spin multiplets. However, the magnetic-dipole selection rule forbids transitions between states with different multiplicity. Therefore, such an undertaking is usually only possible using neutrons [19]. However, Figs. 2 and 3 clearly show that  $J$  can be estimated on the basis of zfs of the lowest lying multiplet. Due to the resultant S-mixing, it may be feasible to observe inter-spin-state EPR transitions directly via far-infrared techniques.

This work is supported by the National Science Foundation, DMR-0239481 and DMR-0506946.

---

corresponding author, Email: hill@phys.u.edu

- [1] R. S. Edwards et al, J. Appl. Phys. 93, 7807 (2003).
- [2] C. K. Kim et al, J. Appl. Phys. 97, 10M 501 (2005).
- [3] E.-C. Yang et al, Polyhedron 22, 1727 (2003).
- [4] E.-C. Yang et al, Inorg. Chem. 44, 3827 (2005).
- [5] E.-C. Yang et al, Inorg. Chem. 45, 529 (2006).
- [6] D. Gatteschi and R. Sessoli, Angew. Chem. 42, 268 (2003).
- [7] E. delBarco et al, Phys. Rev. Lett. 93, 157202 (2004).
- [8] L. Bokacheva, A. D. Kent, and M. A. Walters, Phys. Rev. Lett. 85, 4803 (2000).

- [9] E. delBarco et al., *J. Low Temp. Phys.* 140, 119 (2005).  
[10] K. Park et al., *J. Appl. Phys.* 97, 10M 505 (2005).  
[11] S. Carretta et al., *Phys. Rev. Lett.* 92, 207205 (2004).  
[12] S. Hill et al., *Science* 302, 1015 (2003).  
[13] C. Raghunathan et al., *Phys. Rev. B* 64, 064419 (2001).  
[14] E. delBarco et al., *J. Low Temp. Phys.* 140, 119 (2005).  
[15] N. Chakov et al., *J. Am. Chem. Soc.* 128, 6975 (2006).  
[16] M. Nakano et al. (unpublished).  
[17] A. Wilson et al. (unpublished).  
[18] K. Petukhov et al., *Phys. Rev. B* 70, 054426 (2004).  
[19] S. Carretta et al., *Phys. Rev. B* 73, 144425 (2006).